

Urea-glycerol system: Liquid associated structure studied by dielectric spectroscopy

Marc-Aurele Brun,^{*} Yoshihito Hayashi,[†] Yoichi Katsumoto, Shinji Omori, and Akio Yasuda

Life Science Laboratory, Materials Laboratories, Sony Corporation, Sony Bioinformatics Center, Tokyo Medical and Dental University, Bunkyo-ku, Tokyo 113-8510, Japan

(Received 10 November 2006; revised manuscript received 16 April 2007; published 25 May 2007; publisher error corrected 21 June 2007)

Dielectric measurements of urea-glycerol mixtures were taken over a wide range of urea concentrations (up to 7.6M) and temperatures (from 20 to 80 °C). The dielectric properties begin to change as the urea passes a critical molar fraction, which is independent of temperature and corresponds to a ratio of two urea molecules to seven of glycerol. Our dielectric data support a cluster containing nine molecules of glycerol, which is consistent with neutron-scattering data from the literature. Upon addition of urea, two of the glycerol molecules are substituted with urea to form urea-glycerol coclusters.

DOI: [10.1103/PhysRevB.75.174209](https://doi.org/10.1103/PhysRevB.75.174209)

PACS number(s): 61.20.Lc, 77.22.Gm

I. INTRODUCTION

Pure liquid glycerol has been extensively studied for many years, mainly with regard to its good glass-forming abilities, but also in the domain of protein stabilization and conservation.¹⁻⁴ Still, its associated liquid structure is not yet clearly understood. In fact, a great variety of experimental or simulation techniques have been carried out from dielectric measurement to quasioptical methods and x-ray or neutron scattering, along with molecular dynamics or mode coupling theory simulations.⁵⁻³³ However, these studies have not led to a conclusive understanding of the relation between the microscopic structure of liquid glycerol and its macroscopic properties. In fact, a large number of authors agree on the existence of a short-range order in the hydrogen-bonded (H-bonded) network of liquid glycerol. However, the characteristic distance of this short-range order and the number of molecules participating remain a source of discussion. In parallel, a great number of models and theories based on quite different mechanisms have been proposed to explain the experimental data.

Urea has also been studied in detail, mostly with regard to its protein denaturation properties and its impact on water structure.^{34,35} In spite of these numerous works, the mechanisms of protein denaturation by urea remain unclear.

As far as we know, there have been no published studies on glycerol and urea mixtures. As these two molecules have similar size and H-bonding abilities, but opposite effects on protein structure, we decided to investigate the properties of the mixture. Herein, we describe the results and propose a mechanism for the evolution of the dielectric properties of the mixture over a wide range of concentrations and temperatures (60 K range). The mechanism involves a plausible structure for the dielectric unit in pure glycerol, hereinafter referred to as the glycerol cluster, which is transformed into a glycerol-urea cocluster upon addition of urea.

The experimental techniques are introduced in Sec. II, before a description of the results in Sec. III. In Sec. IV, our model is described in detail, along with other supporting arguments. Section V then summarizes our conclusions.

II. EXPERIMENTAL TECHNIQUES

Pure glycerol (99.9%) was purchased from Wako Chemicals and pure urea from MP Biomedicals. The mixtures were

prepared in a glovebox to prevent water absorption and then sealed in Mighty vials. The vials were further sealed with Parafilm before mixing of the solutions using a standard magnetic stirrer. This operation could take up to two days at room temperature. To speed this up and also to get a rough idea of the evolution of saturation concentration with temperature, we heated the samples in an oven to a maximum temperature of 120 °C. This process resulted in clear solutions for the samples unsaturated at room temperature. For the samples that were saturated at room temperature, particles of urea were visible. A noticeable exception was the most concentrated system. In this system, the urea crystallized at room temperature, so two very distinct phases could be observed: solid urea crystals and a liquid glycerol-urea solution. Over the whole urea concentration range, the density increased by 1%, as measured at 25 °C using a density measurement system (DMA 4500, Anton Paar).

Then, in the glovebox, we transferred some of each solution into Eppendorf tubes. This was done at high temperature (≈ 60 °C, after approximately 20 min in the oven at 100 °C). In this way, homogeneous solutions (no visible heterogeneity) could be obtained even at the highest concentrations. The obtained samples were then ready for measurement. At temperatures from 20 to 50 °C, time domain reflectometry³⁶ (20 MHz–10 GHz) with a Parafilm-sealed cell was used. These results were combined with air measurements as a reference to obtain the complex permittivity of the samples. The temperature control was as precise as 0.1 °C. The quality of the complex permittivity data was not sufficient for fittings below 12 MHz and over 1 GHz. These limits were a result of the multiple reflections effect through the cable (low frequency) and an instrument limitation (high frequency). For higher temperatures (60–80 °C), a vector network analyzer (200 MHz–40 GHz) was used. As the temperature could not be precisely controlled (error of 4.5 °C estimated at 70 °C) with this system, these data were not used for quantitative discussion or fitting. Mostly, these data allowed us to check the influence of the considerable variation in saturation concentration (from $\approx 3.5M$ at room temperature to $\approx 6M$ at ≈ 100 °C). The fitting procedure is described in detail in Sec. III B. Briefly, the algorithm is based on simultaneous least-squares minimization of the mean deviations from the measured values for the real and imaginary parts of the complex permittivity.

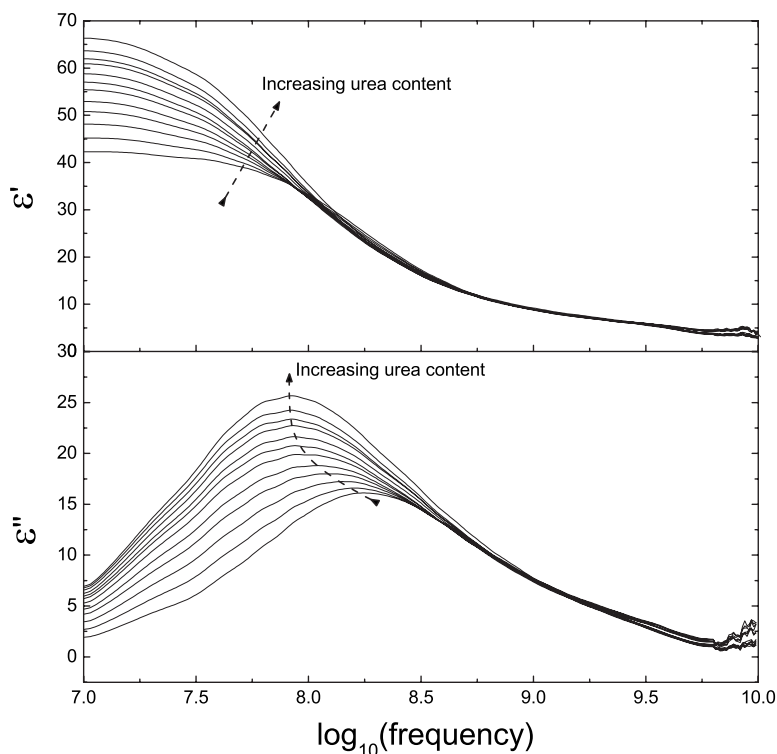


FIG. 1. Dielectric increment (top) and loss (bottom) at 30 °C with increasing urea concentration from pure glycerol up to a urea concentration of 6.2M (step $\approx 0.5M$). Data are shown for frequencies in the range 10 MHz–10 GHz, but the useful range for quantitative interpretation is limited to 12 MHz–1 GHz.

III. EXPERIMENTAL RESULTS AND ANALYSIS

A. Raw spectra and initial analysis

Figure 1 shows the real permittivity and loss at a temperature of 30 °C with increasing urea concentration. Between two successive curves, the urea concentration increases by approximately 0.5M. The spectra are qualitatively similar over the entire temperature range (20–80 °C).

In Fig. 1, one can identify two different domains of urea concentration in terms of the influence of a further addition of urea. At lower concentrations, addition of urea induces a shift in the position of the relaxation peak toward lower frequency and an increase in the dielectric increment. At higher concentrations, addition of urea mainly induces an increase in the dielectric increment, without a noticeable shift in the peak position.

This behavior is much more apparent in Fig. 2, where the peak position and peak value are plotted as a function of urea molar fraction over the entire temperature range (20–80 °C). From these data, we can extract a critical urea molar fraction x_{uc} . This critical value is not correlated with temperature, which indicates that it has no relation to the saturation concentration ($\approx 3.5M$ at room temperature).

This critical molar fraction $x_{uc} = 0.22$ – 0.23 corresponds to a condition where there are two molecules of urea for seven molecules of glycerol. This ratio is used as the starting point for the model we introduce in Sec. IV.

B. Fitting of data

A natural approach to further data analysis is to fit the real and imaginary permittivities. This gives us more information about the processes that occur and how they combine to gen-

erate the observed peak. For pure glycerol, it is known that the main dielectric relaxation process is well described by a Cole-Davidson function,^{37,38} which is equivalent to the Havriliak-Negami function with $\alpha=1$:

$$\hat{\epsilon} - \epsilon_{\infty} = \frac{\Delta\epsilon}{[1 + (j\omega\tau)^{\alpha}]^{\beta}},$$

where j is the imaginary unit, ω is the angular frequency, ϵ_{∞} is the limiting high-frequency permittivity, $\Delta\epsilon$ is the dielectric strength, τ is the relaxation time, and α and β lead to symmetric and asymmetric broadenings of the relaxation function, respectively.

First, we tried to fit our data using only one Havriliak-Negami (HN) process. In this case, as can be seen in Fig. 3, α and β strongly depend on the urea molar fraction. In fact, the sharp decrease in α , simultaneous with the increase in β , can be explained by the existence of a second, slower relaxation process. As this process gains importance, a second loss peak would appear on the low-frequency side of the pure glycerol loss peak. This would induce an artificial symmetrization (β approaching 1) and a consequent broadening (α decreases) of the loss curve. This interpretation is supported by the fact that the minimum α and the maximum β occur at a molar fraction where a relaxation process induced by urea can be reasonably expected ($x_u \approx 0.1$, see Fig. 4).

According to the previous analysis, we can say that the observed loss curve results from the superposition of two relaxation processes. As a hypothesis for fitting, we assumed that the pure glycerol cluster relaxation was not modified by the addition of urea. Therefore, one of the processes would correspond to the pure glycerol relaxation while the other would correspond to the relaxation of the urea-glycerol co-cluster. Thus, we fixed the characteristics of the pure glycerol

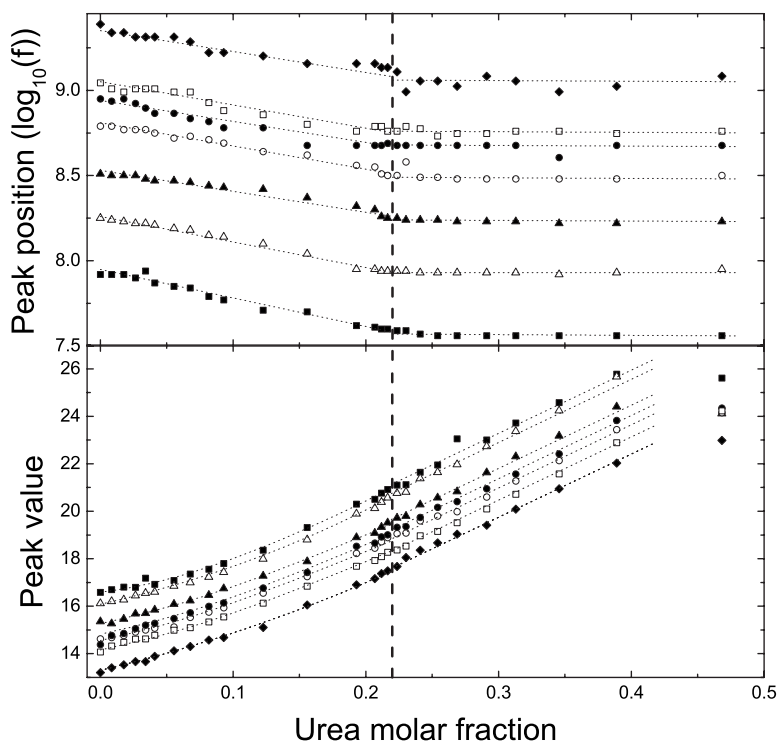


FIG. 2. The different symbols represent temperatures of 20 °C (solid squares), 30 °C (open triangles), 40 °C (solid triangles), 50 °C (open circles), 60 °C (solid circles), 70 °C (open squares), and 80 °C (solid diamonds). Top: the critical molar fraction (roughly indicated by the vertical dashed line) is clearly visible as the peak position reaches a constant value. Bottom: the evolution of the peak value also exhibits this criticality as it changes from a second-order polynomial region to a linear region (the dotted lines are just guides for the eyes).

cluster relaxation according to our pure glycerol data ($\tau = 1.2$ ns at 30 °C; $\alpha=1$ and $\beta=0.69$, constant from 20 to 50 °C), which were in good agreement with previously published values.^{37,38} For the cocluster, only the relaxation time was fixed. This value was extracted from the fits of solutions at urea molar fractions close to the critical value, where the contribution of the pure glycerol process becomes insignificant. Figure 4 shows a typical fit at an intermediate concentration where both cluster populations produce a similar dielectric increment. The good quality of the fits over the entire urea concentration range validates our initial hypothesis. Among the fitting parameters, the dielectric strengths and shape parameters (α and β) of the cocluster need more detailed consideration.

For urea molar fractions between 0.1 and x_{uc} , the values of α and β are stable and represent well the properties of the cocluster relaxation with the following values:

$$\alpha \approx 0.88, \quad \beta \approx 0.77.$$

At lower molar fractions, the small contribution of the cocluster relaxation prevents any precise determination of these parameters. Indeed, the shape of the peak is mainly determined by the relaxation properties of the pure glycerol clusters. Thus, the dispersion of α and β merely reflects the errors in the determination of the fitting parameters over this range. Above the critical molar fraction, α monotonously increases to reach a value of 0.95, while β decreases down to 0.72. This evolution can be reasonably explained by a corresponding evolution of the relaxation properties of the cocluster in this high-concentration range. For the moment, we do not have any consistent explanation for the behavior in this range and focus here on the behavior up to the critical molar fraction, which we model in the next section.

As for the dielectric strengths, represented in Fig. 5, and their evolution with urea concentration, the behavior is quite straightforward: the dielectric strength due to relaxation of the glycerol cluster decreases while the dielectric strength due to cocluster relaxation becomes predominant. Still, we should note that this evolution is linear, which will be of considerable importance in Sec. IV C. A critical molar fraction $x_{uc}=0.22-0.23$ (corresponding to a concentration of 3.3M) is again observed, as the dielectric strength corresponding to pure glycerol reaches zero and the increase in dielectric strength of the cocluster attenuates.

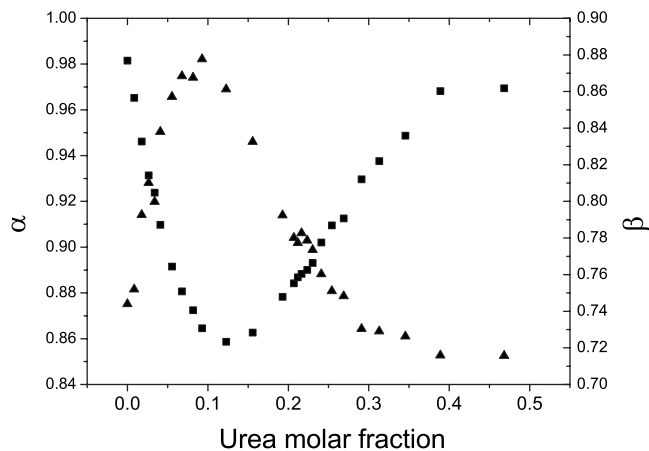


FIG. 3. Evolution of α (squares) and β (triangles) with urea molar fraction for data taken at 30 °C and fitted using only one HN process. The nonmonotonous evolution can be interpreted as an indication that two HN processes are required to describe the behavior (see text for more details).

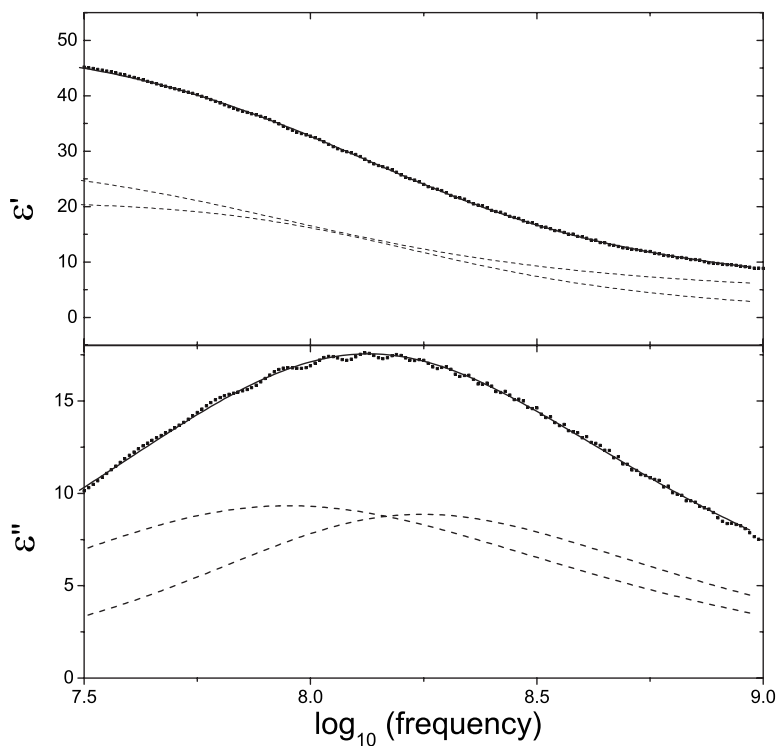


FIG. 4. Fits of the dielectric increment (top) and loss (bottom) at a molar fraction of 0.093 ($T=30\text{ }^{\circ}\text{C}$). The solid line is the sum of the individual HN fitting contributions (dashed lines), and the square symbols indicate the experimental data points. The characteristic parameters for the two HN processes are, for the pure glycerol clusters, $\Delta\epsilon=21$, $\tau=1.2\text{ ns}$, $\alpha=1$, and $\beta=0.69$ (only $\Delta\epsilon$ is varied over the entire concentration range), for the coclusters, $\Delta\epsilon=25.1$, $\tau=2.257\text{ ns}$, $\alpha=0.88$, $\beta=0.77$, and $\epsilon_{\infty}=3.95$ (only τ is fixed).

IV. DISCUSSION

We propose here the structures for the glycerol cluster, i.e., the elementary unit in the dielectric relaxation process, and the cocluster formed with urea.

A. Discussion of raw dielectric data

Considering our data, we noted the existence of a critical molar fraction corresponding to a ratio of two urea molecules

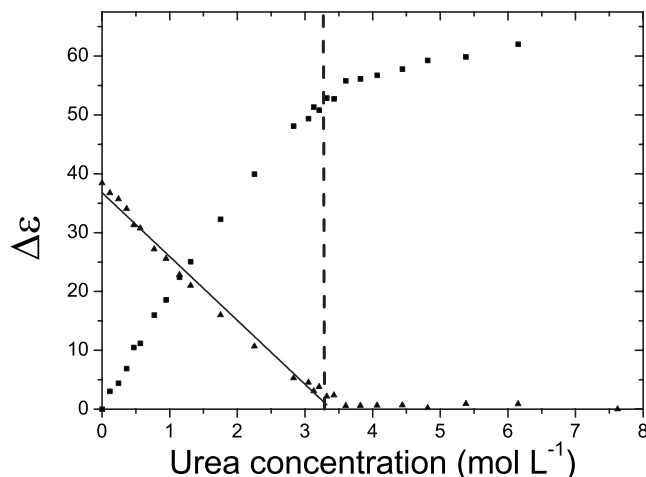


FIG. 5. Dielectric strength, fitting parameter for the pure glycerol cluster (triangles) and cocluster (squares) relaxation processes, as a function of the urea molar concentration at $30\text{ }^{\circ}\text{C}$. The linear fit of the pure glycerol dielectric strength (solid line) is shown to illustrate the argument developed in Sec IV C. The ratio r of the slope to the intersection, as defined in Sec. IV C, is $r=-\frac{-10.9}{36.8}=0.296M^{-1}$.

to seven molecules of glycerol. By a similar reasoning as developed by Mashimo *et al.*,³⁹ we deduce that a glycerol cluster must at least consist of nine molecules. This cluster can be substituted by two molecules of urea to form a cocluster consisting of two urea and seven glycerol molecules.

B. Further evidence from literature

In order to demonstrate our model, we first interpret the experimental data from Garawi *et al.*⁹ confirmed by various molecular-dynamics simulations^{10,23,24,31} in relation to our dielectric data. Figure 6 shows the raw data for $d_L(r)$ as

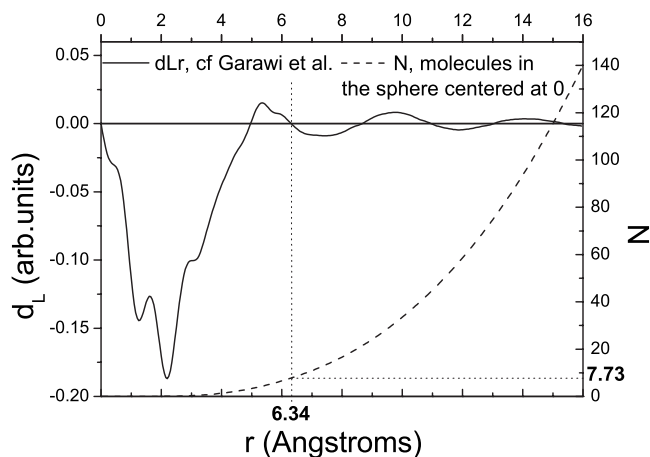


FIG. 6. Data from Garawi *et al.* (Ref. 9), (solid line) and the corresponding number of glycerol molecules as a function of distance from the center molecule (dashed line) calculated using Eq. (1). The dotted lines indicate the size of the dielectric cluster and the number of glycerol molecules included within it.

given in the original paper (obtained for liquid glycerol at 296 K),⁹ along with the calculated number of glycerol molecules as a function of the distance from the center molecule.

To calculate the number of molecules within the cluster, we assumed that the so-called mixed intermolecular correlation factor⁹ $g(r)$ was identifiable to the center-of-mass correlation factor. Thus, we used the following formula, which assumes a spherical symmetry:

$$d_L(r) = 4\pi r \rho_M [g(r) - 1],$$

$$\rho(r) = \rho_M g(r) = \frac{d_L(r)}{4\pi} + \rho_M,$$

$$N(R) = \int_0^R 4\pi r^2 \rho_M g(r) dr, \quad (1)$$

where ρ_M is the average density (or macroscopic density) and r (or R) is the distance from the center molecule. The meaning and relevance of using $d_L(r)$ and $g(r)$ to describe the neutron-scattering data are detailed in Ref. 9.

According to Garawi *et al.*, the peak centered at about 5 Å represents molecules which are orientationally correlated to the central one. This view is supported by the presence of detailed structures in this peak. Indeed, these structures are considered by some authors to be representative of H-bonding-induced orientation correlation.⁴⁰ From a dielectric point of view, we thus claim that this peak is representative of molecules belonging to the same cluster as the central molecule. Integrating over a distance of approximately 6.3 Å, which corresponds to the perimeter of this first high-density ring [$d_L(r) > 0$], we obtain eight molecules. If the central molecule is included, the number of molecules of glycerol in the cluster is 9.

In addition, we considered the work of Arndt *et al.*¹⁴ From dielectric measurements of glass-forming liquid in nanopores, the authors study the effect of confinement on the dynamic glass transition properties. For measurements of glycerol, they obtain a relaxation rate that is identical to bulk values for temperatures down to 190 K and a pore size down to 25 Å (diameter). To analyze the data more precisely, they use a theory based on the existence of two categories of molecules, namely, bulklike molecules and interfacial molecules. The authors finally claim that bulklike behavior occurs in subvolumes as small as 7 Å (diameter) with an interfacial layer of 9 Å, although they themselves noted that these sizes are based on a very rough estimation. Thus, our estimation of a glycerol cluster size of 12.6 Å (diameter) is still in good agreement with their report.

C. Fitted dielectric data and final validity test

In addition to the above evidence, we performed a test to confirm the validity of our model using the values obtained from fitting.

In general, the measured dielectric increment can be related to the number of clusters per unit volume by a simple proportionality relation as follows:

$$\Delta\varepsilon = nC,$$

TABLE I. Values of the ratio r at various temperatures.

T (°C) ^a	20	30	40	50
r (M^{-1})	0.292	0.295	0.281	0.289

^aData for temperatures over 50 °C were not included as the fittings of these data, and the corresponding r values were not very accurate.

where $\Delta\varepsilon$ is the measured dielectric strength, C is a proportionality constant, and n is the number of dielectric units (clusters) per unit volume.

Using the results presented in the Appendix, we can test the validity of our model by fitting a linear regression of the dielectric increment below x_{uc} , as shown in Fig. 5. In this way, we obtain the ratios of the slope to the intercept, as listed in Table I. The very good agreement between these values and those calculated using our model ($0.30M^{-1}$) confirms the model's validity.

V. CONCLUSION

In conclusion, we have proposed a reasonable model for transformation of a glycerol cluster into a glycerol-urea co-cluster with increasing urea concentration. In our model, each cluster consists of nine molecules, with two of the glycerol molecules substituted with urea in the cocluster. Besides our own data, this model is supported by various literature data, including neutron-scattering data and dielectric spectroscopy data for nanopores. A final test of the validity of the model using parameters extracted from fitted data confirmed that the model correctly describes the data below the critical molar fraction x_{uc} . Despite its simplicity, the model is consistent with experimental data from very different sources, which provide additional validation in our opinion. The behavior of the glycerol-urea system above x_{uc} (increase in dielectric increment without a shift in peak position) remains unclear. We will work toward clarifying this in the future.

APPENDIX: DIELECTRIC STRENGTH AND UREA CONCENTRATION

If we consider the concentrations of urea and glycerol, u and g , respectively, then, according to our model, we have the following relations:

$$n_{CO} = \frac{u}{2},$$

$$n_G = \frac{\left(g - \frac{7u}{2}\right)}{9}, \quad (A1)$$

where CO and G refer to the cocluster and the pure glycerol cluster, respectively.

We also have a linear relation between the urea and glycerol concentrations:

$$g = -au + g_0,$$

where a and g_0 (pure glycerol concentration) can be determined experimentally by linear fitting or calculated using the following equations:

$$a = \frac{d_g M_u}{d_u M_g},$$

$$g_0 = \frac{d_g}{M_g},$$

where the indices g and u refer to glycerol and urea, respectively, d is the density, and M is the molecular weight. At 25 °C, we obtain

$$a = 0.62,$$

$$g_0 = 13.7. \quad (\text{A2})$$

Experimentally, we have the following at room temperature:

$$a = 0.66,$$

$$g_0 = 13.65. \quad (\text{A3})$$

Thus, Eq. (A1) becomes

$$n_G = \frac{\left(-a - \frac{7}{2}\right)u}{9} + \frac{g_0}{9}.$$

Thus, we should have $r = -\frac{-a-7/2}{g_0} = 0.30M^{-1}$ from Eq. (A2) and $r = 0.31 M^{-1}$ from Eq. (A3).

*Electronic address: xmarcaurele.brun@jp.sony.com

†Electronic address: yoshihito.hayashi@jp.sony.com

¹S. Decordt, J. Avila, M. Hendrickx, and P. Tobback, *Biotechnology* **44**, 859 (1994).

²S. Jain and J. Ahluwalia, *Thermochim. Acta* **302**, 17 (1997).

³T. Knubovets, J. J. Osterhout, P. J. Connolly, and A. M. Klibanov, *Proc. Natl. Acad. Sci. U.S.A.* **96**, 1262 (1999).

⁴G. Caliskan, A. Kisliuk, A. M. Tsai, C. L. Soles, and A. P. Sokolov, *J. Non-Cryst. Solids* **307**, 887 (2002).

⁵G. E. McDuffie and T. A. Litovitz, *J. Chem. Phys.* **37**, 1699 (1962).

⁶H. van Koningsveld, *Recl. Trav. Chim. Pays-Bas* **87**, 243 (1968).

⁷M. Wolfe and J. Jonas, *J. Chem. Phys.* **71**, 3252 (1979).

⁸D. C. C. R. N. Joarder and J. C. Dore, *Mol. Phys.* **58**, 337 (1986).

⁹M. Garawi, J. C. Dore, and D. C. Champeney, *Mol. Phys.* **62**, 475 (1987).

¹⁰L. J. Root and F. Stillinger, *J. Chem. Phys.* **90**, 1200 (1989).

¹¹N. P. Malomuzh and S. B. Pelishenko, *Phys. Lett. A* **154**, 269 (1991).

¹²S. Kojima, *Phys. Rev. B* **47**, 2924 (1993).

¹³U. Mohanty, *J. Chem. Phys.* **100**, 5905 (1994).

¹⁴M. Arndt, R. Stannarius, W. Gorbatschow, and F. Kremer, *Phys. Rev. E* **54**, 5377 (1996).

¹⁵T. Uchino and T. Yoko, *Science* **26**, 480 (1996).

¹⁶S. Sarkar and R. N. Joarder, *Phys. Lett. A* **222**, 195 (1996).

¹⁷J. Wuttke, W. Petry, and S. Pouget, *J. Chem. Phys.* **105**, 5177 (1996).

¹⁸F. J. Bermejo, A. Criado, A. de Andres, E. Enciso, and H. Schober, *Phys. Rev. B* **53**, 5259 (1996).

¹⁹C. M. Roland and K. L. Ngai, *J. Chem. Phys.* **106**, 1187 (1997).

²⁰J. A. Padro, L. Saiz, and E. Guardia, *J. Mol. Struct.* **416**, 243 (1997).

²¹S. V. Lishchuk and N. P. Malomuzh, *J. Chem. Phys.* **106**, 6160 (1997).

²²S. V. Lishchuk and N. P. Malomuzh, *Chem. Phys. Lett.* **309**, 307 (1999).

²³R. Chelli, P. Procacci, G. Cardini, R. G. D. Valle, and S. Califano, *Phys. Chem. Chem. Phys.* **1**, 871 (1999).

²⁴R. Chelli, P. Procacci, G. Cardini, and S. Califano, *Phys. Chem. Chem. Phys.* **1**, 879 (1999).

²⁵G. M. Plavnik and T. P. Puryaeva, *Colloid J.* **63**, 467 (2000).

²⁶W. T. M. Mooij, B. P. van Eijck, and J. Kroon, *J. Am. Chem. Soc.* **122**, 3500 (2000).

²⁷S. Sudo, M. Shimomura, N. Shinyashiki, and S. Yagihara, *J. Non-Cryst. Solids* **307–310**, 356 (2002).

²⁸E. Guardia, J. Marti, J. A. Padro, L. Saiz, and A. V. Komolkin, *J. Mol. Liq.* **96**, 3 (2002).

²⁹I. V. Blazhnov, N. P. Malomuzh, and S. V. Lishchuk, *J. Chem. Phys.* **121**, 6435 (2004).

³⁰E. L. Mertz, *J. Phys. Chem. A* **109**, 44 (2005).

³¹J. Blicke, F. Affouard, P. Bordat, A. Lerbret, and M. Descamps, *Chem. Phys.* **317**, 253 (2005).

³²J. C. Phillips, *Phys. Rev. B* **73**, 024210 (2006).

³³U. Buchenau, M. Ohl, and A. Wischnewski, *J. Chem. Phys.* **124**, 094505 (2006).

³⁴J. G. Grdadolnik and Y. Marechal, *J. Mol. Struct.* **615**, 177 (2002).

³⁵A. K. Soper, E. W. Castner, and A. Luzar, *Biophys. Chem.* **105**, 649 (2003).

³⁶J. G. Berberian and E. King, *J. Non-Cryst. Solids* **305**, 10 (2002).

³⁷F. Kremer, *J. Non-Cryst. Solids* **305**, 1 (2002).

³⁸A. Puzenko, Y. Hayashi, Y. E. Ryabovand, I. Balin, Y. Feldman, U. Kaatze, and R. Behrends, *J. Phys. Chem. B* **109**, 6031 (2005).

³⁹S. Mashimo, T. Umehara, and H. Redlin, *J. Chem. Phys.* **95**, 6257 (1991).

⁴⁰R. L. Leheny, N. Menon, S. R. Nagel, and D. L. Price, *J. Chem. Phys.* **105**, 7783 (1996).